


Serine proteases mediate leukocyte recruitment and hepatic microvascular injury in the acute phase following extended hepatectomy

Yunjie Zhang¹  | Patrick Huber¹ | Marc Praetner¹ | Alice Zöllner¹ | Lesca Holdt² | Andrej Khandoga³ | Maximilian Lerchenberger³

¹Walter-Brendel Centre of Experimental Medicine, Ludwig-Maximilians-Universität Munich, Munich, Germany

²Institute of Laboratory Medicine, LMU University Hospitals, Ludwig-Maximilians-Universität Munich, Munich, Germany

³Department of General, Visceral, and Transplant Surgery, LMU University Hospitals, Ludwig-Maximilians-Universität Munich, Munich, Germany

Correspondence

Maximilian Lerchenberger, Department of General, Visceral, and Transplant Surgery, LMU University Hospitals, Ludwig-Maximilians-Universität Munich, Marchioninistraße 15, 81377 Munich, Germany.

Email: maximilian.lerchenberger@med.uni-muenchen.de

Funding information

China Scholarship Council; FöFoLe; Friedrich-Baur-Stiftung

Abstract

Objective: Post-hepatectomy liver failure (PHLF) is the main limitation of extended liver resection. The molecular mechanism and the role of leukocytes in the development of PHLF remain to be unveiled. We aimed to address the impact of serine proteases (SPs) on the acute phase after liver resection by intravitaly analyzing leukocyte recruitment and changes in hemodynamics and microcirculation of the liver.

Methods: C57BL/6 mice undergoing 60% partial hepatectomy were treated with aprotinin (broad-spectrum SP inhibitor), tranexamic acid (plasmin inhibitor), or vehicle. Sham-operated animals served as controls. In vivo fluorescence microscopy was used to quantify leukocyte-endothelial interactions immediately after, as well as 120 min after partial hepatectomy in postsinusoidal venules, along with measurement of sinusoidal perfusion rate and postsinusoidal shear rate. Recruitment of leukocytes, neutrophils, T cells, and parameters of liver injury were assessed in tissue/blood samples.

Results: Leukocyte recruitment, sinusoidal perfusion failure rate, and shear rate were significantly increased in mice after 60% partial hepatectomy compared to sham-operated animals. The inhibition of SPs or plasmin significantly attenuated leukocyte recruitment and improved the perfusion rate in the remnant liver. ICAM-1 expression and neutrophil recruitment significantly increased after 60% partial hepatectomy and were strongly reduced by plasmin inhibition.

Conclusions: Endothelial activation and leukocyte recruitment in the liver in response to the increment of sinusoidal shear rate were hallmarks in the acute phase after liver resection. SPs mediated leukocyte recruitment and contributed to the impairment of sinusoidal perfusion in an ICAM-1-dependent manner in the acute phase after liver resection.

Abbreviations: ALT, alanine aminotransferase; AST, aspartate aminotransferase; FITC, fluorescein isothiocyanate; ICAM-1, intercellular adhesion molecule-1; MAP, mean arterial pressure; PH, partial hepatectomy; PHLF, post-hepatectomy liver failure; SEM, standard error of the mean; SP, serine protease; TNF- α , tumor necrosis factor- α ; TXA, tranexamic acid; uPA, urokinase-type Plg activator.

This is an open access article under the terms of the [Creative Commons Attribution-NonCommercial](https://creativecommons.org/licenses/by-nc/4.0/) License, which permits use, distribution and reproduction in any medium, provided the original work is properly cited and is not used for commercial purposes.

© 2022 The Authors. *Microcirculation* published by John Wiley & Sons Ltd.

KEYWORDS

hepatectomy, intravital microscopy, liver microcirculation, small-for-size syndrome

1 | BACKGROUND

Liver resection is recognized as a standard surgical procedure treating primary liver tumors, hepatic metastasis,¹ and various end-stage liver diseases requiring liver transplantation.^{2,3} Nevertheless, this approach is largely limited because excessive resection might cause post-hepatectomy liver failure (PHLF) associated with a mortality rate up to 30%.⁴ The incidence of PHLF is reported from 1.2% to 32% according to different centers⁴ and is correlated with the extent of liver resection.⁵ Surgical approaches to limit the portal perfusion showed preventive effects, such as transjugular intrahepatic portosystemic shunts, splenectomy, and splenic artery embolization, but these were accompanied by various postoperative and intraoperative complications.^{6,7} Hence, more effort should be made to understand the pathophysiological mechanism for developing efficient therapeutic strategies.

A general hypothesis concerning the pathophysiological mechanism is the “portal hyperperfusion.” Under physiological conditions, an autoregulating mechanism called “hepatic arterial buffer response” compensates for increased hepatic perfusion. This mechanism is regulated by the adenosine, a dilator of the hepatic artery, secreted at a consistent rate in liver sinusoids. An increased portal blood flow caused by, for example, hypervolemia results in a “washout” of adenosine. The contraction of the hepatic artery thus follows the decreased concentration of adenosine. However, this mechanism fails to compensate for the massive portal inflow in the context of extended hepatectomy. The persistent hepatic hyperperfusion causes an increment in hepatic microvascular shear stress.⁸ Excessive shear stress and lowered oxygen supply due to the contraction of the hepatic artery leads to endothelial injury and necrosis,⁹ which hinders liver function and regeneration.¹⁰

In response to the change of shear stress, immune cells play a major role in the process of both injury and subsequent regeneration. The recruited neutrophils contribute to the hepatic parenchymal injury facilitated by releasing matrix metalloproteinases-9 after liver resection in mice.¹¹ The neutrophils can also contribute to liver regeneration by interacting with intercellular adhesion molecule-1 (ICAM-1), which leads to the release of pro-regenerative cytokines, such as tumor necrosis factor- α (TNF- α) and Interleukin-6 from the Kupffer cells.¹² An animal study using mice model showed that Kupffer cells mediated liver injury after partial liver transplantation via the pathway of TNF- α .¹³ However, the spatial and temporal details of leukocyte recruitment following microcirculatory change in the early phase after liver resection are yet to be clarified. Recent studies focused mainly on the impact of immune response on liver regeneration, whereas limited effort has been made on the pathophysiological mechanism of early-phase liver injury after partial liver resection.

Serine proteases (SPs) are endopeptidases and their main function is to cleave peptide bonds in proteins. Plasmin, one of the most prominent SPs, is formed in the liver as a zymogen known as plasminogen (Plg). Plg is synthesized in the liver and predominantly activated by the physiological activators urokinase-type Plg activator (uPA) or tissue-type Plg activator. After activation, plasmin cleaves insoluble fibrin clots into a soluble fibrin degradation product. Beyond the fibrinolytic properties, recent studies revealed its versatility to mediate the processes of both inflammation and regeneration in various liver diseases.^{14–17} In the context of hepatectomy, early activity of Plg activators was reported in humans following hepatectomy.^{18,19} An *in vivo* chemotaxis assay using a mice cremaster model from our group suggested the inhibition of SPs or plasmin suppressed intravascular accumulation and transmigration of neutrophils.^{20,21}

The clinical evidence of increased SP activity after hepatectomy and the engagement of SPs in the development of inflammation implies that SPs, specifically plasmin, might play important roles in initiating liver injury immediately after liver resection. Therefore, we hypothesized that SPs could regulate acute hepatic injury after extended hepatectomy. The current study aimed to clarify the pathological mechanism of acute hepatic injury regarding SPs using intravital investigation focused on the microcirculatory changes.

2 | METHODS AND MATERIALS

2.1 | Animals

Female C57BL/6 mice (10–14 weeks of age, approximately 20–25 g body weight) were used (Charles River). Mice were housed in a temperature-controlled room with about 22°C and with humidity of about 60% on a 12-h light–dark cycle, with free access to food and water. The acclimatization of the animals was 1 week before the experiment. Animal experiments were performed according to the German legislation on the protection of animals (Protocol Nr.: 02-17-132). Our group has investigated several mouse strains in pilot studies. The constant size of the left liver lobe of age-related female C57BL/6 mice thereby provided reproducible and suitable *in vivo* imaging quality (no published data available). Notably, the inflammatory response was reported to be different in male and female mice.^{22,23}

Animals were divided into four groups; (1) control group ($n = 11$): animals receiving only sham operation in treatment of 0.9% NaCl as a vehicle; (2) 60% partial hepatectomy (PH) group ($n = 11$): animals receiving approximately 60% PH in treatment of 0.9% NaCl as a vehicle; (3) 60% PH+aprotinin group ($n = 11$): animals receiving approximately 60% PH in treatment of aprotinin; and (4) 60% PH+tranexamic acid group ($n = 11$): animals receiving approximately

60% PH in treatment of tranexamic acid (TXA). All groups received intravital microscopic investigations.

2.2 | Surgical procedures

General anesthesia was induced via intraperitoneal injection of midazolam/medetomidine/fentanyl with a dosage of 5, 0.5, and 0.05 mg/kg, respectively. Partial doses were administered hourly to maintain anesthesia. The surgical tolerance of the mice was proven using interdigital reflex. The animals were placed in a supine position on a heating pad. An anal probe was inserted to measure the body temperature, which was kept at $37 \pm 1^\circ\text{C}$. Oxygen (1 L/min, $\text{FiO}_2 = 0.35$) was supplied with a mask throughout the procedures. Polyethylene catheters (PE 50, ID 0.28 mm; Portex) were inserted into the left jugular vein and carotid artery. Mean arterial pressure (MAP) and heart rate were continuously monitored using Powerlab (ADInstrument) for intraoperative monitoring. The 60% PH was performed by ligating and resecting the median lobe, right upper and lower lobes using a modification of technique reported by Tomohide Hori et al.²⁴ Blood lost during the surgery was around 10 μl , excluding resident blood in the resected liver lobes.

2.3 | Reagents

The effective doses were tested and determined according to our published work.^{20,21} Aprotinin, a broad-spectrum SP inhibitor (100000 KIU/kg/h, Sigma-Aldrich) or TXA, a plasmin inhibitor (100 mg/kg/h, Sigma-Aldrich) were infused intravenously (i.v.) starting from 5 min before hepatectomy (injection duration: 5 min) in two separate intervention groups with 60% PH. Both reagents were dissolved following the manufacturer's instructions. Fluorescein isothiocyanate (FITC)-labeled Dextran (100 μl , 5%, MW 150000, Sigma-Aldrich) was administered i.v. to visualize liver perfusion. Leukocytes were visualized by an i.v. application of rhodamine 6G (0.05%, 50 μl , Sigma-Aldrich).

2.4 | Intravital fluorescence microscopy

Intravital fluorescence microscopy was performed using a modified Leitz-Orthoplan microscope as described previously.²⁵ Rhodamine 6G and FITC were applied intravenously. FluoSpheres™ Sulfate Microspheres, 2.0 μm , yellow-Green fluorescent (505/515), 2% solids (10 μl diluted in 50 μl Saline, Invitrogen) were injected i.v. allowing the determination of centerline blood velocity in postsinusoidal venules. Using an N2 filter block (excitation: 530–560 nm, emission: >580 nm, Leitz), five to seven randomly chosen postsinusoidal venules with diameters ranging from 20 to 40 μm were observed by 30 s each filter. Using the I2/3 filter block (excitation: 450–490 nm, emission: >515 nm; Leitz), ten fields of randomly chosen, non-adjacent sinusoids were observed by 5 s.

2.5 | Microcirculatory analysis

The videotaped images were digitalized and analyzed off-line by frame-to-frame analysis using ImageJ.²⁶ The following parameters were analyzed: (1) the average diameter of postsinusoidal venules; (2) the average number of rolling leukocytes (the leukocytes rolling on the targeting vessel wall and passing the observed area of a postsinusoidal venule with a length of 150 μm in 30 s); (3) the average number of firmly adherent leukocytes (the leukocytes located in the observed area and without moving at least 20 s within 30-s observation time); (4) the average centerline blood flow velocity (shear rate of postsinusoidal venules wall, according to the Newtonian definition [$\gamma = 8 \times \text{centerline velocity} / 1.6 / \text{diameter}$]) where the centerline velocity was measured using MtrackJ plugin²⁷; (5) perfusion failure rate: percentage of sinusoids with no perfusion vs. all sinusoids per acinus.

2.6 | Blood samples

The blood taken from the vena cava was immediately centrifuged at 3000 g for 5 min. Serum samples were stored at -80°C . Total bilirubin, serum aspartate aminotransferase (AST), and alanine aminotransferase (ALT) levels were measured with an automated analyzer (AU 5800; Beckman Coulter) using standardized test systems (HiCo GOT and HiCo GPT; Roche Applied Sciences).

2.7 | Immunohistochemistry (IHC)

The liver remnant was collected at the end of each experiment. After conservation, paraffin sections were performed with a slice thickness of 4 μm at the level of 50% of the liver lobe thickness. Antigen retrieval was performed with a 20 min 95°C water bath with citrate buffer, pH 6.0. CD45 antibody (1:200, Cell Signaling Technology, #70257), ICAM-1 antibody (1:2000, Abcam, 179707), Ly-6G antibody (1:1000, Biolegend, 127602), and CD3 antibody (1:150 Abcam, 16669) were used as primary antibody. Secondary detection was performed by Super Sensitive detecting system (BioGenex).

CD45, Ly-6G, and CD3 positive cells in sinusoids were counted in 10 high-power fields (at microscope magnification $\times 400$) in a blinded manner. One tissue section was examined per animal. The adherent leukocytes in postsinusoidal venules were analyzed using intravital microscopy. Thus, intravascularly localized positive cells were not counted.²⁸ Analysis of ICAM-1 expression was performed semi-quantitatively in a blinded fashion with a grading system of 0–3: 0, no staining; 1, weak staining; 2, mild staining; and 3, strong staining.²⁸

2.8 | Statistics

All data analyses were performed with a statistical software package (SigmaPlot 13.0, Systat Software). The Kolmogorov–Smirnov

test was performed to verify the normality. If confirmed, one-way analysis of variance with Tukey test was used for the intergroup statistical comparison. If not confirmed, analysis of variance on ranks followed by the Student–Newman–Keuls method was used to estimate stochastic probability in intergroup comparison. The data are presented in mean values \pm standard error of the mean (SEM).

3 | RESULTS

3.1 | Macrohemodynamic parameters

The MAP of all groups of animals receiving PH was not significantly different from the MAP in sham-operated animals of 74.6 ± 1.7 mmHg (Group receiving 60% PH and vehicle treatment: 70.8 ± 0.8 mmHg; group receiving 60% PH and aprotinin treatment: 67.8 ± 2.3 mmHg; group receiving 60% PH and TXA treatment: 71.8 ± 1.4 mmHg). Intermittent MAP increment was found immediately after i.v. injection of inhibitors or vehicle, which was quickly renormalized before hepatectomy (Figures S1A and S2). Aprotinin caused a significantly larger increment (9.22 ± 1.32 mmHg) compared to animals treated with TXA (5.64 ± 1.45 mmHg) or vehicle-treated animals receiving sham operation or 60% PH (3.58 ± 0.60 and 3.78 ± 0.96 mmHg, respectively, Figure S1B).

3.2 | Intravital parameters

3.2.1 | Rolling leukocytes

A significant increase in the number of rolling leukocytes in post-sinusoidal venules was detected immediately ($9.1 \pm 0.9/30s$) and after 2 h ($14.9 \pm 1.2/30s$) in animals after 60% PH compared to sham-operated animals ($3.7 \pm 0.5/30s$ and $4.9 \pm 0.4/30s$, respectively, Figure 1A,B). In animals undergoing 60% PH, the numbers of rolling leukocytes were significantly decreased after treatment with aprotinin (baseline $6.7 \pm 0.3/30s$; 2 h $9.7 \pm 1.0/30s$) or TXA (baseline $4.1 \pm 0.5/30s$; 2 h $8.7 \pm 0.5/30s$) compared to vehicle-treated animals (Figure 1B). No significant difference in the number of rolling leukocytes was detected between TXA-treated animals undergoing 60% PH and sham-operated animals in the baseline measurement.

3.2.2 | Firmly adherent leukocytes

The mean number of firmly adherent leukocytes in sham-operated animals was $25.1 \pm 6.4/mm^2$ at baseline. This number significantly increased to $120.4 \pm 13.4/mm^2$ in animals undergoing 60% PH. After 2 h, the number of firmly adherent leukocytes in animals that underwent 60% PH was dramatically increased with a threefold

difference ($535.6 \pm 28.7/mm^2$) compared to sham-operated animals ($171.7 \pm 30.6/mm^2$).

The numbers of firmly adherent leukocytes were significantly decreased immediately after PH in animals treated with aprotinin ($22.2 \pm 5.4/mm^2$) or TXA ($19.12 \pm 5.3/mm^2$). Also, the increment in adherent cells caused by PH 2 h after resection was significantly suppressed in the presence of aprotinin ($199.4 \pm 22.2/mm^2$) or TXA ($106.9 \pm 17.4/mm^2$) compared to vehicle-treated animals (Figure 1C).

3.2.3 | Perfusion failure rate

A significant difference in perfusion failure rate was detected in animals that underwent 60% PH group at baseline ($15.9 \pm 1.3\%$) and 2 h after resection ($21.8 \pm 1.0\%$) compared to sham-operated animals ($6.9 \pm 0.5\%$ and $12.5 \pm 1.2\%$, respectively). Two hours after PH, the perfusion failure rates in the animals treated with aprotinin or TXA were slightly higher ($15.6 \pm 0.9\%$ and $14.2 \pm 0.9\%$, respectively) without significance than in sham-operated animals (Figure 2A,B).

3.2.4 | Shear rate

The shear rate in postsinusoidal venules in the sham group had a mean of $164.2 \pm 12.7/s$ at baseline and $143.3 \pm 10.6/s$ after 2 h. The shear rate was significantly elevated in vehicle-treated animals undergoing 60% PH, both at baseline and 2 h ($229.0 \pm 15.8/s$ and $209.5 \pm 13.8/s$, respectively). The shear rate was slightly lower in the baseline measurement ($198.7 \pm 13.2/s$) and significantly lower 2 h after hepatectomy ($164.0 \pm 12.9/s$) after treatment with the broad-spectrum inhibitor of SPs compared to the vehicle-treated animals receiving 60% PH. In contrast, the shear rate significantly increased with the specific inhibition of plasmin (baseline $264.5 \pm 16.8/s$ and 2 h $249.3 \pm 17.4/s$, Figure 2c) compared to the vehicle-treated animals undergoing 60% PH.

3.2.5 | Bilirubin, AST and ALT

Concentration of total bilirubin in serum increased significantly after PH (sham 0.72 ± 0.19 mg/dl; 60% PH 1.23 ± 0.19 mg/dl). Aprotinin or TXA treatment significantly decreased the level of total bilirubin after PH (aprotinin 0.88 ± 0.15 ; TXA 0.54 ± 0.08 mg/dl, Figure 3A).

A large increase in levels of transaminases (AST 1453 ± 133 ; ALT 974 ± 75 U/L) was found in the vehicle-treated animals undergoing 60% PH compared with the sham-operated animals (AST 339 ± 95 ; ALT 195 ± 59 U/L, Figure 3B). The serum levels of transaminases significantly decreased in the group undergoing 60% PH and treated with aprotinin (AST 995 ± 137 ; ALT 704 ± 111 U/L) or TXA (AST 1041 ± 95 ; ALT 657 ± 62 U/L) compared to the vehicle-treated animals undergoing 60% PH.

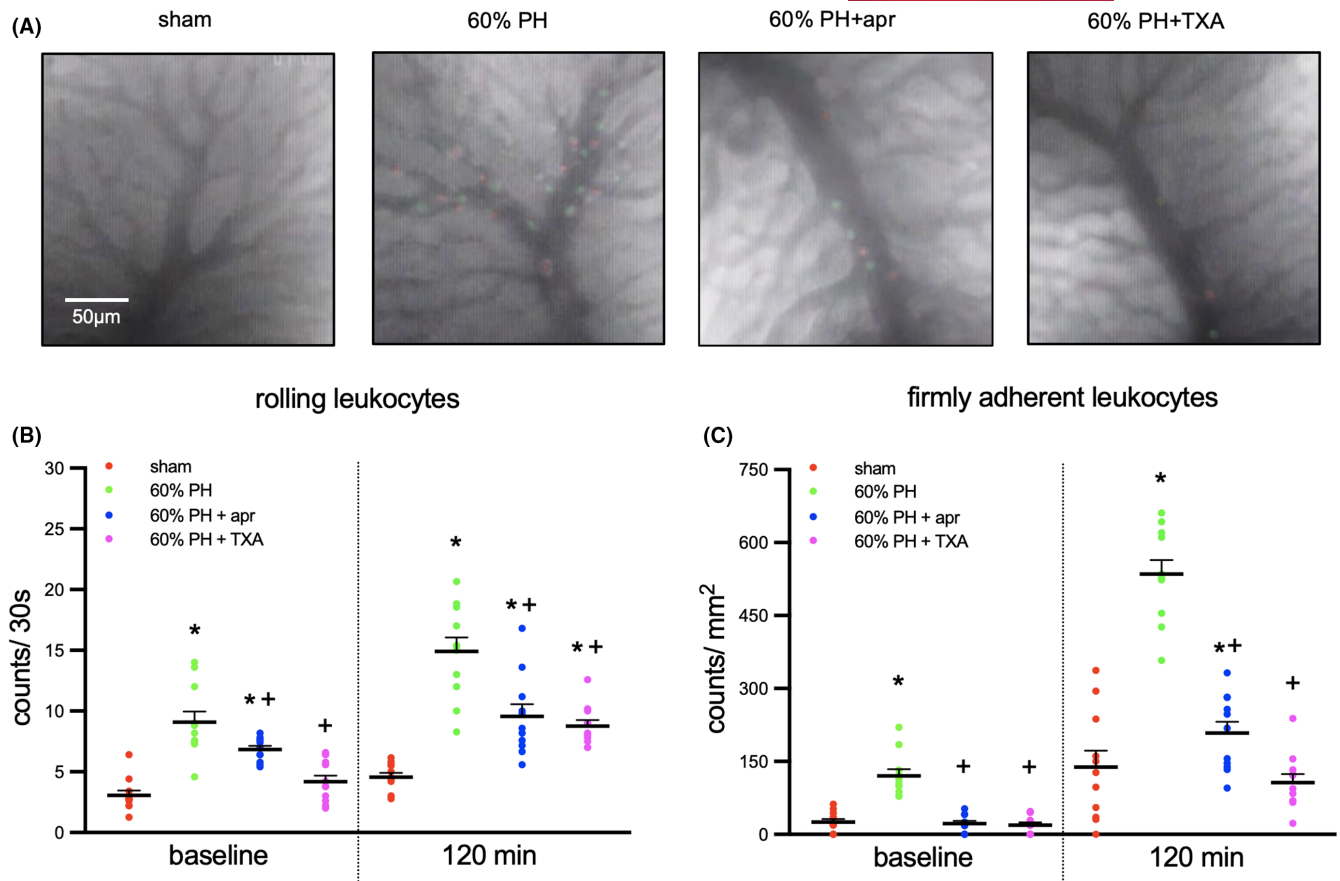


FIGURE 1 In vivo quantification of leukocyte-endothelial interaction after 60% PH. (A) Images of fluorescence microscope showing rolling (marked with green) and firmly adherent leukocytes (marked with red) in postsinusoidal venules in different groups. The example from each group is one frame from a 30-s video (10 frames per second), in which the green-marked leukocytes passed the venule with a rolling behavior and red-marked leukocytes stayed stagnant. (B, C) The numbers of rolling and firmly adherent leukocytes increased immediately after 60% PH. The applications of aprotinin or TXA ameliorated this increment after 60% PH. $n = 11$ animals per group, mean \pm SEM. PH, partial hepatectomy; apr, aprotinin; TXA, tranexamic acid. * $p < .05$, versus sham-operated group; + $p < .05$, versus 60% PH group.

3.3 | Immunohistochemistry

The subpopulation of the leukocytes in the liver after 60% PH. A significant increase in the number of leukocytes (CD45⁺) and neutrophils (Ly-6g⁺, Figure 4) were found in hepatic sinusoids 2 h after PH. In animals treated with aprotinin or TXA, the number of recruited leukocytes was significantly reduced. Notably, the number of recruited neutrophils in sinusoids was found significantly decreased after treatment with TXA, but not with broad-spectrum inhibition of SPs.

The number of T cells (CD3⁺) was higher in animals undergoing 60% PH than in the sham-operated animals, but the difference was not significant. After the treatment with aprotinin and TXA, the number of T cells decreased without a significant difference (Figure 4C,F).

3.3.1 | ICAM-1

The immunohistochemical analysis showed significant overexpression of ICAM-1 in both hepatic sinusoids and hepatic venules after PH. The expression of ICAM-1 was found significantly lowered in

both hepatic sinusoids and postsinusoidal after the treatment with aprotinin or TXA (Figure 5A,B).

4 | DISCUSSION

Facing an increasing demand for living donor liver transplantation²⁹ and curative resection of hepatic metastasis from colon cancer, effective preventions and treatments of PHLF become an urgent appeal to improve the outcome and reduce life-threatening complications after extended hepatectomy.³⁰ This poses the importance of better understanding the pathophysiological mechanism of PHLF. Prior work documented the functions of immune cells regarding liver injury and regeneration after extended hepatectomy.^{11,13,31,32} However, the detailed picture of the immune mechanism in the acute phase following liver resection is still missing. This study focused on the leukocyte-endothelial interaction and microhemodynamic alteration within a 2-h after the hepatectomy.

A similar murine model using Sprague–Dawley rat with stepwise PH also investigated by intravital fluorescence microscopy was

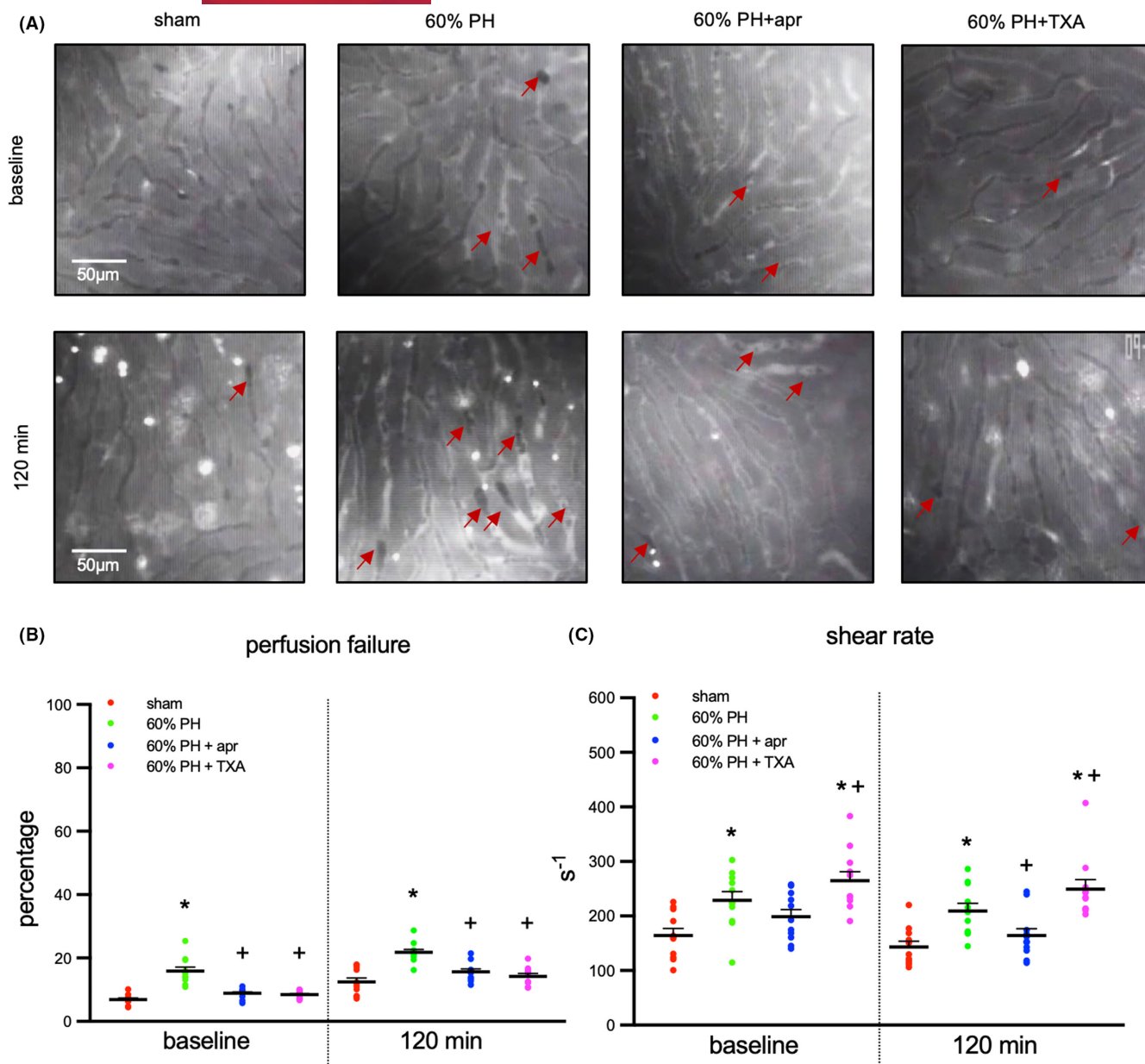


FIGURE 2 In vivo analysis of the microvascular injury and the shear rate in postsinusoidal venules after PH. (A) Images of the FITC channel showed a significant perfusion rate of the remnant liver after 60% PH. The red arrowheads represent the non-perfused sinusoids, which were observed using video data. The dots with a high signal 2 h after PH are the fluorescent beads phagocytosed by the Kupffer cells. (B) Significantly increased perfusion failure was found immediately after 60% PHs. The microcirculation was improved after the application of aprotinin and TXA. (c) Shear stress increased immediately after PH and showed different changes after applying aprotinin or TXA. $n = 11$ animals per group, mean \pm SEM. PH, partial hepatectomy; apr, aprotinin; TXA, tranexamic acid. * $p < .05$, versus sham-operated group; + $p < .05$, versus 60% PH group.

reported by Dold et al.³³ We adapted this model and used C57BL/6 mice with a similar surgical technique to intravitaly observe the initial endothelial activation and microvascular injury in response to the change of shear rate in the acute phase after PH. This model enabled us to create the acute pathophysiological situation after liver resection and to perform an intravital observation and analysis on the remnant liver so that the behavioral change of the cellular immune and microcirculatory failure could be quantified with reproducibility. This advantage could not be achieved using human objects.

Our results brought the first evidence that the hepatic endothelium was immediately activated in response to the excessive shear rate following extended hepatectomy. This phenomenon is reflected by an initial augmentation of the rolling and firm adherent leukocytes in postsinusoidal venules. Our results also confirmed the theory proposed by Sato et al that the increment of shear stress could facilitate the leukocyte transmigration into parenchyma.³⁴ Attenuated leukocyte-endothelial interaction was found starting from the baseline measurement after the broad-spectrum inhibition of SPs

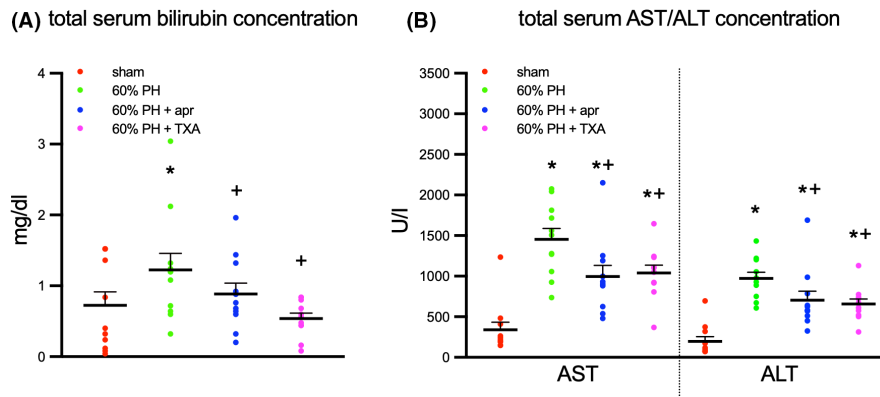


FIGURE 3 Liver function and injury reflected by bilirubin level and enzyme activity. (A) Disorders of bilirubin clearance were found after 60%PH. The liver function was improved after applying aprotinin and TXA after 60% PH. (B) Serum activity of the liver enzyme showed a significant necrotic injury 2h after 60% PH. Aprotinin or TXA ameliorated liver injury after 60% PH. PH, partial hepatectomy; apr, aprotinin; TXA, tranexamic acid; AST, serum aspartate aminotransferase; ALT, alanine aminotransferase. $n = 11$ animals per group, mean + SEM. * $p < .05$, versus sham-operated group; + $p < .05$, versus 60% PH group.

by aprotinin. Interestingly, despite the shear rate increment, fewer rolling and firmly adherent leukocytes were found in the postsinusoidal venules in the TXA-treated animals undergoing 60% PH. This implied that shear stress might facilitate the leukocyte-endothelial interaction in a plasmin-dependent manner after liver resection. This finding also indicated that SPs, especially plasmin, could mediate the initial leukocyte recruitment in response to the excessive shear rate in the remnant liver.

The results of baseline measurements indicated that the hepatic microcirculation was impaired before the leukocytes were recruited into the hepatic parenchyma. Early perfusion failure was found immediately after liver resection. A normal function of sinusoidal perfusion is essential for the following liver regeneration after PH,³⁵ which poses the importance to address the pathophysiological mechanism of endothelial injury in liver microcirculation. Structural impairment of sinusoids was found along with the increment of portal vein pressure in studies using partial liver transplantation models.^{36,37} Sinusoidal hyperperfusion and severe endothelial injury were reported following 90% PH in the rats reported by Li et al.³⁸ A significant perfusion failure was documented only in 90% PH using a stepwise hepatectomy in rats, according to Dold et al.³³

Of interest, our results showed that the SPs or plasmin inhibition improved sinusoidal perfusion in the context of extended hepatectomy. Aprotinin and TXA are known as inhibitors of fibrinolysis,³⁹ and TXA is widely used in the prevention of bleeding from trauma and surgeries.⁴⁰ The inhibition of plasmin can cause fewer fibrin clots degradation. This could theoretically induce the formation of thrombi and deteriorate the microperfusion. However, our finding indicated that plasmin engaged rather in the inflammatory process than the fibrinolytic process in the remnant mouse liver where no direct surgical trauma happened after liver resection. This agrees with the finding from a prospective phase-II trial that TXA does not affect systemic fibrinolysis following PH.⁴¹

Furthermore, the plasmin inhibition and broad-spectrum SP inhibition retained the liver function and ameliorated liver injury in the acute phase after PH reflect by the serum concentration of AST and ALT. This amelioration of liver injury might be explained by the reduced number of recruited leukocytes. However, the quantification of rolling and firmly adherent leukocytes only partially reflect the extent of leukocyte transmigration. Thus, the number of transmigrated leukocytes in the hepatic parenchyma and its subpopulation were investigated using IHC analysis. A significantly increased number of recruited leukocytes were detected in the hepatic parenchyma, which supported the *in vivo* finding. The number of neutrophils was quantified to address the possible cause for liver injury in the acute phase after liver resection because the recruited neutrophils were reported to cause liver injury in different liver diseases directly.^{11,42,43} The neutrophils can release several proteases such as myeloperoxidase, matrix metalloproteinases, and elastases, which induce tissue degradation and necrosis.⁴⁴ The number of recruited neutrophils was found to significantly increased after the vehicle-treated animal undergoing 60% PH. In contrast to the increment of leukocytes and neutrophils, no significant change in the number of T cells was found within 2h after 60% PH. Sato et al also reported that unlike neutrophils, a significantly increased number of CD3⁺ T cells was first found 2 days after PH.⁴⁵

ICAM-1 is a critical molecule to regulate the leukocyte firm adhesion.⁴⁶ The ICAM-1 expression was found to be significantly higher after 60% PH. This might explain the dramatically increased number of firmly adherent leukocytes in vehicle-treated animals after 60% PH from the *in vivo* analysis, and the expanded number of neutrophils in the parenchyma shown in the IHC analysis. Further IHC analysis showed that the ICAM-1 expression (sinusoids and hepatic veins) was reduced by the broad-spectrum inhibitor aprotinin and by the plasmin inhibition from TXA, despite the significant shear rate increased in the presence of TXA.

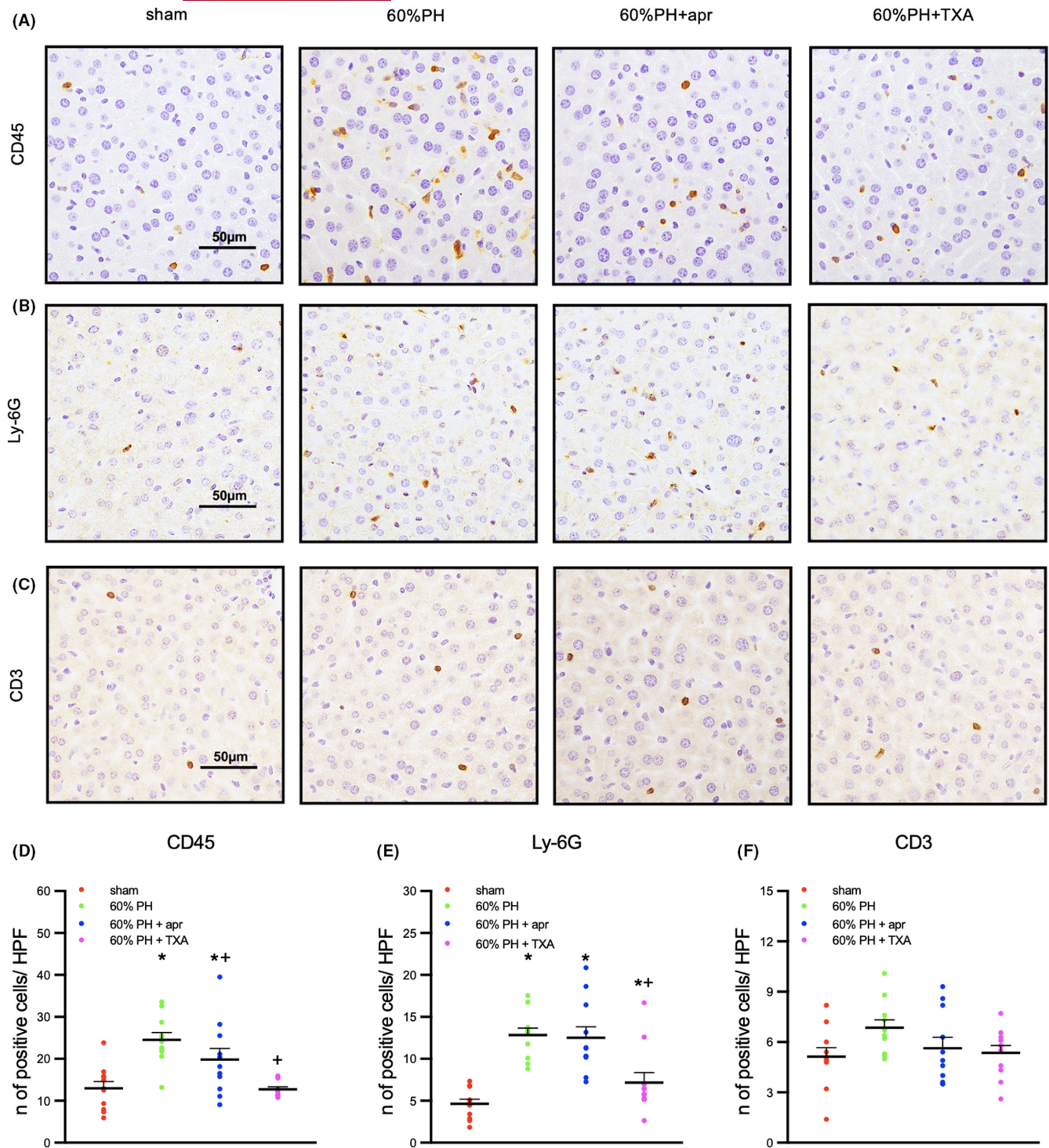


FIGURE 4 Different leukocyte subpopulations quantified using Immunohistochemistry analysis. (A–C) Leukocytes, neutrophils, and T cells were marked with CD45, Ly-6G, and CD3, respectively. (D) The number of leukocytes increased significantly after 60% PH. This increment was significantly suppressed after the treatment with aprotinin or TXA. (E) The number of neutrophils increased significantly after 60% PH. The treatment with TXA but not aprotinin significantly reduced the number of neutrophils. (F) The increase in the number of CD3 positive cells was not significant after 60% PH. $n = 11$ animals per group, mean + SEM. PH, partial hepatectomy; apr, aprotinin; TXA, tranexamic acid; HFP: high-power field * $p < .05$, versus sham-operated group; + $p < .05$, versus 60%-PH group.

The current study had several limitations. Only female C57BL/6 mice were used in our study due to the importance of liver anatomical stability for the quality of the microscopic analyses. The results and conclusions might not apply to both genders,

and further experiments might be required to confirm findings in male mice.

In this study, intravital microscopy enabled us to investigate the microcirculatory alteration immediately after PH. Liver regeneration

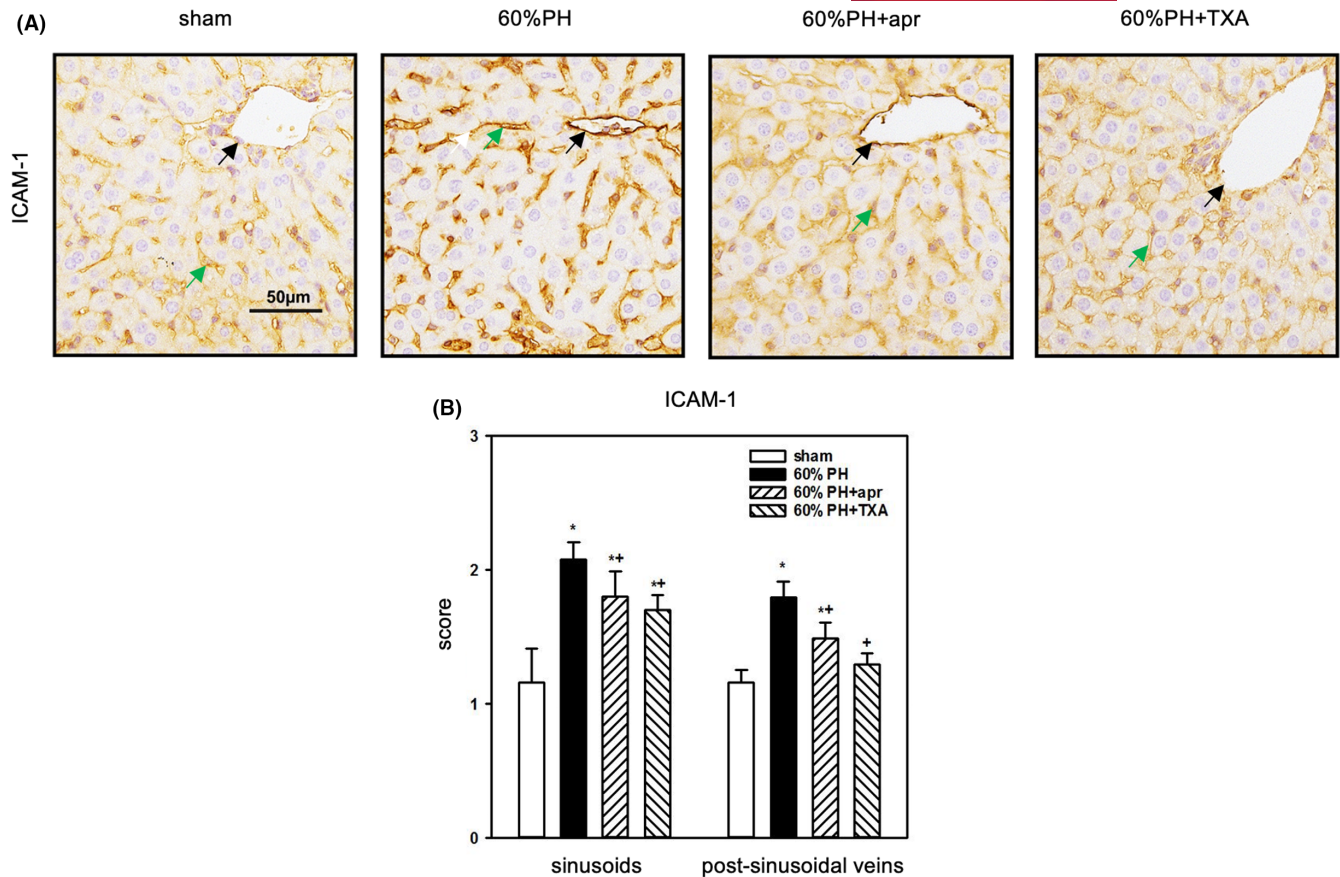


FIGURE 5 Expressions of ICAM-1. (A, B) The ICAM-1 expression was significantly increased after 60% PH. This upregulation was found both in the sinusoids and the hepatic venule wall (marked representatively using green and black arrowheads, respectively). (C, D) The inhibition of SPs or Plasmin significantly suppressed the expression of ICAM-1 both in the sinusoids and the hepatic venule wall. $n = 11$ animals per group, mean \pm SEM. PH, partial hepatectomy; apr, aprotinin; TXA, tranexamic acid. * $p < .05$, versus sham-operated group; + $p < .05$, versus 60% PH group.

was not investigated. Okada et al¹⁵ and Miura et al⁴⁷ reported that the plasmin system regulates liver regeneration. Our findings in the acute phase depicted the role of plasmin in the formation of PHLF. It contributed to early-phase microvascular injury and impairment of liver function. Although the application of TXA and aprotinin showed no significant effect on liver regeneration in the first 2h (data of Ki-67 analysis not showed), the long-term effect on liver regeneration still needs to be investigated.

Taken together, it was demonstrated in this study that initial leukocyte-endothelial interaction and early perfusion failure were two hallmarks occurring immediately after PH. SPs play an important role in leukocyte recruitment and early liver injury. The inhibition of plasmin lowered ICAM-1-facilitated neutrophil recruitment and ameliorates liver injury after PH.

4.1 | Perspectives

An *in vivo* microscopic technique was used to unveil the dynamic insight of hepatic microcirculatory changes and recruitment of the leukocyte in the remnant liver in an acute phase after liver resection using a murine model. Moreover, the first data were required

showing that serine proteases, especially plasmin, can mediate this acute pathologic process.

AUTHOR CONTRIBUTIONS

Yunjie Zhang, Patrick Huber, Marc Praetner, and Alice Zöllner participated in *in vivo* and *in vitro* experiments. Yunjie Zhang and M L participated in statistical analysis and wrote the manuscript. Lesca Holdt participated in laboratory analysis. Maximilian Lerchenberger and Andrej Khandoga participated in the conception and design of the study.

ACKNOWLEDGMENTS

The authors would like to thank Mrs. Britta Clementine Pauli and Mrs. Dorothea Fichtl for their technical assistance. This study was funded by grants of FöFoLe and Friedrich-Baur-Stiftung to Maximilian Lerchenberger and China Scholarship Council to Yunjie Zhang. Open Access funding enabled and organized by Projekt DEAL.

CONFLICT OF INTEREST

The authors declare that they have no conflict of interest. Animal experiments were performed according to the German legislation on the protection of animals (Protocol Nr.: 02-17-132).

DATA AVAILABILITY STATEMENT

The authors confirm that the data supporting the findings of this study are available in the article.

ORCID

Yunjie Zhang  <https://orcid.org/0000-0001-8379-5088>

REFERENCES

- Narita M, Oussoultzoglou E, Bachellier P, Jaeck D, Uemoto S. Post-hepatectomy liver failure in patients with colorectal liver metastases. *Surg Today*. 2015;45:1218-1226.
- Shoreem H, Gad EH, Soliman H, et al. Small for size syndrome difficult dilemma: lessons from 10years single Centre experience in living donor liver transplantation. *World J Hepatol*. 2017;9:930-944.
- Clavien PA, Petrowsky H, DeOliveira ML, Graf R. Strategies for safer liver surgery and partial liver transplantation. *N Engl J Med*. 2007;356:1545-1559.
- Rahbari NN, Garden OJ, Padbury R, et al. Posthepatectomy liver failure: a definition and grading by the international study Group of Liver Surgery (ISGLS). *Surgery*. 2011;149:713-724.
- Clavien PA, Eshmuminov D. Small for size: laboratory perspective. *Liver Transpl*. 2015;21(Suppl 1):S13-S14.
- Saad WE. Transjugular intrahepatic portosystemic shunt before and after liver transplantation. *Semin Intervent Radiol*. 2014;31:243-247.
- Raut V, Alikhanov R, Belghiti J, Uemoto S. Review of the surgical approach to prevent small-for-size syndrome in recipients after left lobe adult LDLT. *Surg Today*. 2014;44:1189-1196.
- Becker D, Hefti M, Schuler MJ, et al. Model assisted analysis of the hepatic arterial buffer response during ex vivo porcine liver perfusion. *IEEE Trans Biomed Eng*. 2020;67:667-678.
- Poisson J, Lemoine S, Boulanger C, et al. Liver sinusoidal endothelial cells: physiology and role in liver diseases. *J Hepatol*. 2017;66:212-227.
- Kohler A, Moller PW, Frey S, et al. Portal hyperperfusion after major liver resection and associated sinusoidal damage is a therapeutic target to protect the remnant liver. *Am J Physiol Gastrointest Liver Physiol*. 2019;317:G264-G274.
- Ohashi N, Hori T, Chen F, et al. Matrix metalloproteinase-9 in the initial injury after hepatectomy in mice. *World J Gastroenterol*. 2013;19:3027-3042.
- Selzner N, Selzner M, Odermatt B, Tian Y, Van Rooijen N, Clavien PA. ICAM-1 triggers liver regeneration through leukocyte recruitment and Kupffer cell-dependent release of TNF-alpha/IL-6 in mice. *Gastroenterology*. 2003;124:692-700.
- Tian Y, Jochum W, Georgiev P, Moritz W, Graf R, Clavien PA. Kupffer cell-dependent TNF-alpha signaling mediates injury in the arterialized small-for-size liver transplantation in the mouse. *Proc Natl Acad Sci USA*. 2006;103:4598-4603.
- Henkel AS, Khan SS, Olivares S, Miyata T, Vaughan DE. Inhibition of plasminogen activator inhibitor 1 attenuates hepatic steatosis but does not prevent progressive nonalcoholic Steatohepatitis in mice. *Hepatol Commun*. 2018;2:1479-1492.
- Okada K, Ueshima S, Imano M, Kataoka K, Matsuo O. The regulation of liver regeneration by the plasmin/alpha 2-antiplasmin system. *J Hepatol*. 2004;40:110-116.
- Avalos-de Leon CG, Jimenez-Castro MB, Cornide-Petronio ME, Casillas-Ramirez A, Peralta C. The role of GLP1 in rat Steatotic and non-Steatotic liver transplantation from Cardiocirculatory death donors. *Cell*. 2019;8:1599.
- Gao S, Silasi-Mansat R, Behar AR, Lupu F, Griffin CT. Excessive plasmin compromises hepatic sinusoidal vascular integrity after acetaminophen overdose. *Hepatology*. 2018;68:1991-2003.
- Mangnall D, Smith K, Bird NC, Majeed AW. Early increases in plasminogen activator activity following partial hepatectomy in humans. *Comp Hepatol*. 2004;3:11.
- Mars WM, Liu ML, Kitson RP, Goldfarb RH, Gabauer MK, Michalopoulos GK. Immediate early detection of urokinase receptor after partial hepatectomy and its implications for initiation of liver regeneration. *Hepatology*. 1995;21:1695-1701.
- Lerchenberger M, Uhl B, Stark K, et al. Matrix metalloproteinases modulate ameoboid-like migration of neutrophils through inflamed interstitial tissue. *Blood*. 2013;122:770-780.
- Reichel CA, Lerchenberger M, Uhl B, et al. Plasmin inhibitors prevent leukocyte accumulation and remodeling events in the postischemic microvasculature. *Plos One*. 2011;6:e17229.
- Angele MK, Knoferl MW, Ayala A, Bland KI, Chaudry IH. Testosterone and estrogen differently effect Th1 and Th2 cytokine release following trauma-haemorrhage. *Cytokine*. 2001;16:22-30.
- Diodato MD, Knoferl MW, Schwacha MG, Bland KI, Chaudry IH. Gender differences in the inflammatory response and survival following haemorrhage and subsequent sepsis. *Cytokine*. 2001;14:162-169.
- Hori T, Ohashi N, Chen F, et al. Simple and reproducible hepatectomy in the mouse using the clip technique. *World J Gastroenterol*. 2012;18:2767-2774.
- Khandoga A, Biberthaler P, Enders G, et al. Platelet adhesion mediated by fibrinogen-intercellular adhesion molecule-1 binding induces tissue injury in the postischemic liver in vivo. *Transplantation*. 2002;74:681-688.
- Schneider CA, Rasband WS, Eliceiri KW. NIH image to ImageJ: 25 years of image analysis. *Nat Methods*. 2012;9:671-675.
- Meijering E, Dzyubachyk O, Smal I. Methods for cell and particle tracking. *Methods Enzymol*. 2012;504:183-200.
- Khandoga A, Kessler JS, Meissner H, et al. Junctional adhesion molecule-a deficiency increases hepatic ischemia-reperfusion injury despite reduction of neutrophil transendothelial migration. *Blood*. 2005;106:725-733.
- Lee SG. A complete treatment of adult living donor liver transplantation: a review of surgical technique and current challenges to expand indication of patients. *Am J Transplant*. 2015;15:17-38.
- Creasy JM, Sadot E, Koerkamp BG, et al. The impact of primary tumor location on long-term survival in patients undergoing hepatic resection for metastatic colon cancer. *Ann Surg Oncol*. 2018;25:431-438.
- Jin X, Zhang Z, Beer-Stolz D, Zimmers TA, Koniaris LG. Interleukin-6 inhibits oxidative injury and necrosis after extreme liver resection. *Hepatology*. 2007;46:802-812.
- Rudich N, Zamir G, Pappo O, et al. Focal liver necrosis appears early after partial hepatectomy and is dependent on T cells and antigen delivery from the gut. *Liver Int*. 2009;29:1273-1284.
- Dold S, Richter S, Kollmar O, et al. Portal hyperperfusion after extended hepatectomy does not induce a hepatic arterial buffer response (HABR) but impairs mitochondrial redox state and hepatocellular oxygenation. *Plos One*. 2015;10:e0141877.
- Sato Y, Tsukada K, Hatakeyama K. Role of shear stress and immune responses in liver regeneration after a partial hepatectomy. *Surg Today*. 1999;29:1-9.
- Greene AK, Wiener S, Puder M, et al. Endothelial-directed hepatic regeneration after partial hepatectomy. *Ann Surg*. 2003;237:530-535.
- Man K, Lo CM, Ng IO, et al. Liver transplantation in rats using small-for-size grafts: a study of hemodynamic and morphological changes. *Arch Surg*. 2001;136:280-285.
- Li J, Liang L, Ma T, et al. Sinusoidal microcirculatory changes after small-for-size liver transplantation in rats. *Transpl Int*. 2010;23:924-933.

38. Li CH, Ge XL, Pan K, Wang PF, Su YN, Zhang AQ. Laser speckle contrast imaging and oxygen to see for assessing microcirculatory liver blood flow changes following different volumes of hepatectomy. *Microvasc Res*. 2017;110:14-23.
39. Moore EE, Moore HB, Gonzalez E, et al. Postinjury fibrinolysis shut-down: rationale for selective tranexamic acid. *J Trauma Acute Care Surg*. 2015;78:S65-S69.
40. Roberts I. Tranexamic acid in trauma: how should we use it? *J Thromb Haemost*. 2015;13(Suppl 1):S195-S199.
41. Karanicolas PJ, Lin Y, Tarshis J, et al. Major liver resection, systemic fibrinolytic activity, and the impact of tranexamic acid. *HPB*. 2016;18:991-999.
42. Rosales C. Neutrophil: a cell with many roles in inflammation or several cell types? *Front Physiol*. 2018;9:113.
43. Yago T, Petrich BG, Zhang N, et al. Blocking neutrophil integrin activation prevents ischemia-reperfusion injury. *J Exp Med*. 2015;212:1267-1281.
44. Oliveira THC, Marques PE, Proost P, Teixeira MMM. Neutrophils: a cornerstone of liver ischemia and reperfusion injury. *Lab Invest*. 2018;98:51-62.
45. Sato Y, Tsukada K, Iiai T, et al. Activation of extrathymic T cells in the liver during liver regeneration following partial hepatectomy. *Immunology*. 1993;78:86-91.
46. Ley K, Laudanna C, Cybulsky MI, Nourshargh S. Getting to the site of inflammation: the leukocyte adhesion cascade updated. *Nat Rev Immunol*. 2007;7:678-689.
47. Miura A, Ishiguro K, Koizumi K, et al. Effects of pharmacological inhibition of plasminogen binding on liver regeneration in rats. *Biosci Biotechnol Biochem*. 2017;81:2105-2111.

SUPPORTING INFORMATION

Additional supporting information can be found online in the Supporting Information section at the end of this article.

How to cite this article: Zhang Y, Huber P, Praetner M, et al. Serine proteases mediate leukocyte recruitment and hepatic microvascular injury in the acute phase following extended hepatectomy. *Microcirculation*. 2023;30:e12796. doi:[10.1111/micc.12796](https://doi.org/10.1111/micc.12796)